

DOI: 10.11973/jxgccl202302012

# 局部堆焊修复 U75V 钢轨的滚动接触磨损特性

容彬<sup>1,2</sup>,汪永强<sup>1,2</sup>,赵火平<sup>1,2,3</sup>,刘少鹏<sup>1,2</sup>,沈明学<sup>1,2,3</sup>

(华东交通大学 1. 载运工具与装备教育部重点实验室, 2. 材料科学与工程学院, 3. 轨道交通基础设施性能监测与保障国家重点实验室, 南昌 330013)

**摘要:** 对未堆焊和局部堆焊 U75V 钢轨试样进行干态+湿态两阶段连续滚动接触磨损试验, 对比分析了 2 种钢轨试样的滚动接触特性及磨损行为。结果表明: 2 种钢轨试样的黏着系数在干态磨损阶段都在 0.60 左右, 进入湿态磨损阶段急剧下降至 0.25 左右; 干态磨损阶段局部堆焊钢轨试样的黏着系数略高于未堆焊钢轨试样, 湿态磨损阶段则相反。局部堆焊钢轨试样的堆焊层主要由马氏体组成, 硬度最高, 磨损表面损伤轻微, 未发现明显裂纹与塑性变形; 热影响区由铁素体、珠光体与马氏体等组织组成, 硬度居中, 磨损后表面粗糙度最大, 塑性变形较大且出现较多大角度扩展的裂纹; 无堆焊区主要由珠光体组成, 硬度最小, 磨损后表面平坦, 塑性变形较明显, 出现少量裂纹。

**关键词:** 钢轨; 堆焊修复; 滚动接触磨损; 塑性变形; 裂纹

中图分类号: TH117

文献标志码: A

文章编号: 1000-3738(2023)02-0067-06

## Rolling Contact Wear Characteristics of U75V Rail Repaired by Local Surfacing

RONG Bin<sup>1,2</sup>, WANG Yongqiang<sup>1,2</sup>, ZHAO Huoping<sup>1,2,3</sup>, LIU Shaopeng<sup>1,2</sup>, SHEN Mingxue<sup>1,2,3</sup>

(1. Key Laboratory of Vehicle and Equipment, Ministry of Education, 2. School of Materials Science and Engineering, 3. National Key Laboratory of Rail Transit Infrastructure Performance Monitoring and Guarantee, East China Jiaotong University, Nanchang 330013, China)

**Abstract:** The dry and wet two-stage continuous rolling contact wear tests were carried out on U75V rail samples without surfacing and with local surfacing. The rolling contact characteristics and wear behavior of the two rail samples were compared and analyzed. The results show that the adhesion coefficients of the two rail samples were both about 0.60 in the dry wear stage, and decreased sharply to about 0.25 into the wet wear stage; the adhesion coefficient of the local surfacing rail sample in the dry wear stage was slightly higher than the un-surfacing rail sample, and the wet wear stage was the opposite. The surfacing layer of the local surfacing rail sample mainly consisted of martensite and had the highest hardness. The wear surface damage of surfacing layer was slight, and no obvious cracks and plastic deformation were found. The heat affected zone was composed of ferrite, pearlite and martensite and the hardness was in the middle. After wear, the surface roughness of the heat affected zone was the largest, the plastic deformation was large and there were many cracks with large expansion angles. The non-surfacing zone was mainly composed of pearlite and the hardness was the lowest. After wear, the surface of the non-surfacing zone was flat, and obvious plastic deformation and a small amount of cracks were found.

**Key words:** rail; surfacing repair; rolling contact wear; plastic deformation; crack

## 0 引言

轮轨间的正常接触是列车牵引与制动的保障, 高速度、大轴重列车的迅猛发展使得钢轨表面的损伤日趋加快且越发严重, 出现如轨头压溃、波浪磨损、弯曲变形、剥离裂纹与局部硌伤等情况。损伤会导致钢轨的不平顺, 使得列车在行驶时的轴向和垂

收稿日期: 2022-01-06; 修订日期: 2022-12-25

基金项目: 国家自然科学基金资助项目(52061012, 51805170); 江西省自然科学基金资助项目(20212ACB214003, 20224ACB204012)

作者简介: 容彬(1997-), 男, 广西钦州人, 硕士研究生

通信作者(导师): 沈明学教授

向加速度骤然增加,从而影响列车上人员的乘坐舒适性,甚至危及行车安全<sup>[1]</sup>。采用合理的表面修复技术对伤损钢轨进行修复,能在保证钢轨正常服役的前提下延长其使用寿命,这对于节约运输成本、保障列车的运营品质具有重要意义<sup>[2-3]</sup>。不同类型的钢轨损伤可以采取不同方式进行修复:损伤深度较浅时一般采用钢轨打磨方式,损伤深度较深则采取切割后焊接方式,而损伤深度介于二者之间时采用堆焊方式<sup>[4]</sup>。

堆焊主要用于轨头的修复,如电弧堆焊可以修复轨头的剥离掉块、滚动接触疲劳裂纹等损伤,并且在处理表层的长距离损伤时具备优势<sup>[5]</sup>。学者们对钢轨堆焊修复及损伤机理进行了深入的探讨与研究:一方面通过现场试验对修复后的钢轨进行堆焊区域的性能测试<sup>[6-7]</sup>,分析堆焊工艺对修复后钢轨的组织与力学性能的影响<sup>[8-11]</sup>;另一方面基于有限元模型对钢轨堆焊部位进行仿真分析,从车辆-轨道耦合动力学的角度研究不同因素对钢轨堆焊区域的塑性变形及应力、应变的影响,如车速、轴重、轨头接头高度及堆焊后钢轨的不平整度等因素<sup>[12-17]</sup>。轮轨一般是滚动接触,车轮以滚动方式通过钢轨焊接区域,然而目前关于钢轨表面堆焊层滚动接触特性及损伤行为的研究鲜见报道。为此,作者对 U75V 钢轨试样表面进行局部堆焊处理并对未堆焊和局部堆

焊 U75V 钢轨进行干态+湿态两阶段连续滚动接触试验,对比分析了未堆焊和局部堆焊钢轨的滚动接触磨损特性、磨损后的微观形貌以及滚动接触磨损机理,拟为钢轨损伤修复提供理论参考。

## 1 试样制备与试验方法

### 1.1 试样制备

试验所用钢轨试样取自 U75V 钢轨轨头,车轮试样取自 CL60 钢车轮踏面,尺寸见图 1;堆焊修复使用的填充焊丝为 0Cr18Ni9 奥氏体不锈钢焊丝。3 种材料的化学成分见表 1。

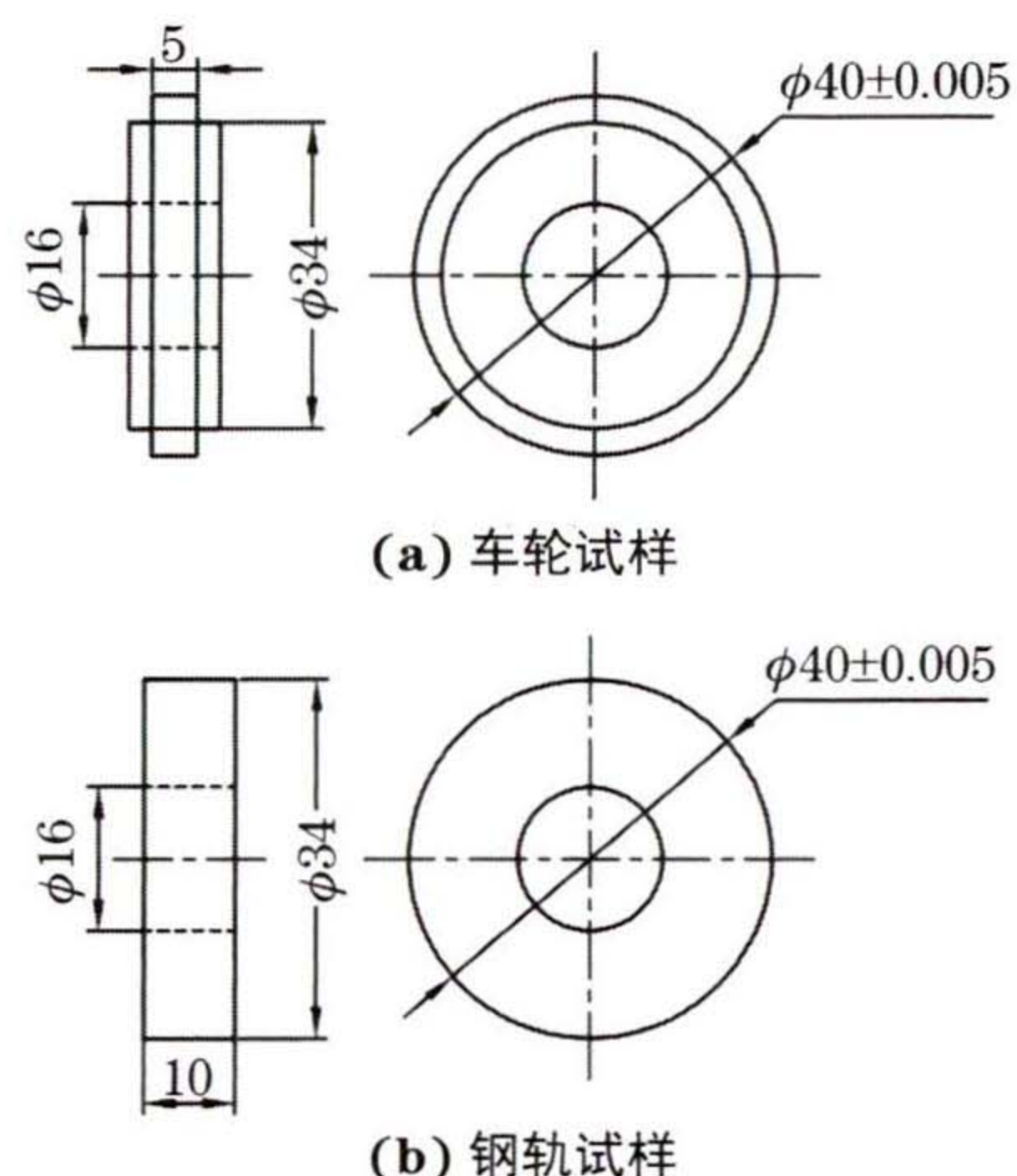


图 1 车轮和钢轨试样的尺寸

Fig. 1 Size of wheel (a) and rail (b) samples

表 1 CL60 钢、U75V 钢和 0Cr18Ni9 不锈钢的化学成分

Table 1 Chemical composition of CL60 steel, U75V steel and 0Cr18Ni9 stainless steel

材料	质量分数/%					
	C	Mn	P	Si	Cr	Ni
CL60 钢	0.57~0.65	0.50~0.80	<0.035	0.17~0.37		
U75V 钢	0.71~0.80	0.75~1.05	<0.030	0.50~0.80		
0Cr18Ni9 不锈钢	≤0.07	≤2.00	≤0.035	≤1.00	17.0~19.0	8.0~11.0

堆焊工艺参数是影响堆焊区显微组织和力学性能的关键因素。根据文献<sup>[18]</sup>确定如下工艺参数:堆焊电流 100 A,堆焊电压 19 V,堆焊速度 25~35 mm·min<sup>-1</sup>。使用 BX1-400 型工业级交流弧焊机设备对 U75V 钢轨试样进行周向三等分堆焊,如图 2 所示。对未堆焊和有堆焊层钢轨试样表面进行磨削和抛光,使其表面粗糙度  $R_a$  达到 0.1 μm。

### 1.2 试验方法

在 JD-DRCF/M 型滚动接触磨损试验台上进行滚动接触磨损试验,上试样为车轮试样,转速为 525 r·min<sup>-1</sup>,下试样分别为未堆焊和局部堆焊钢轨试样,转速为 500 r·min<sup>-1</sup>。为模拟 30 t 轴重重

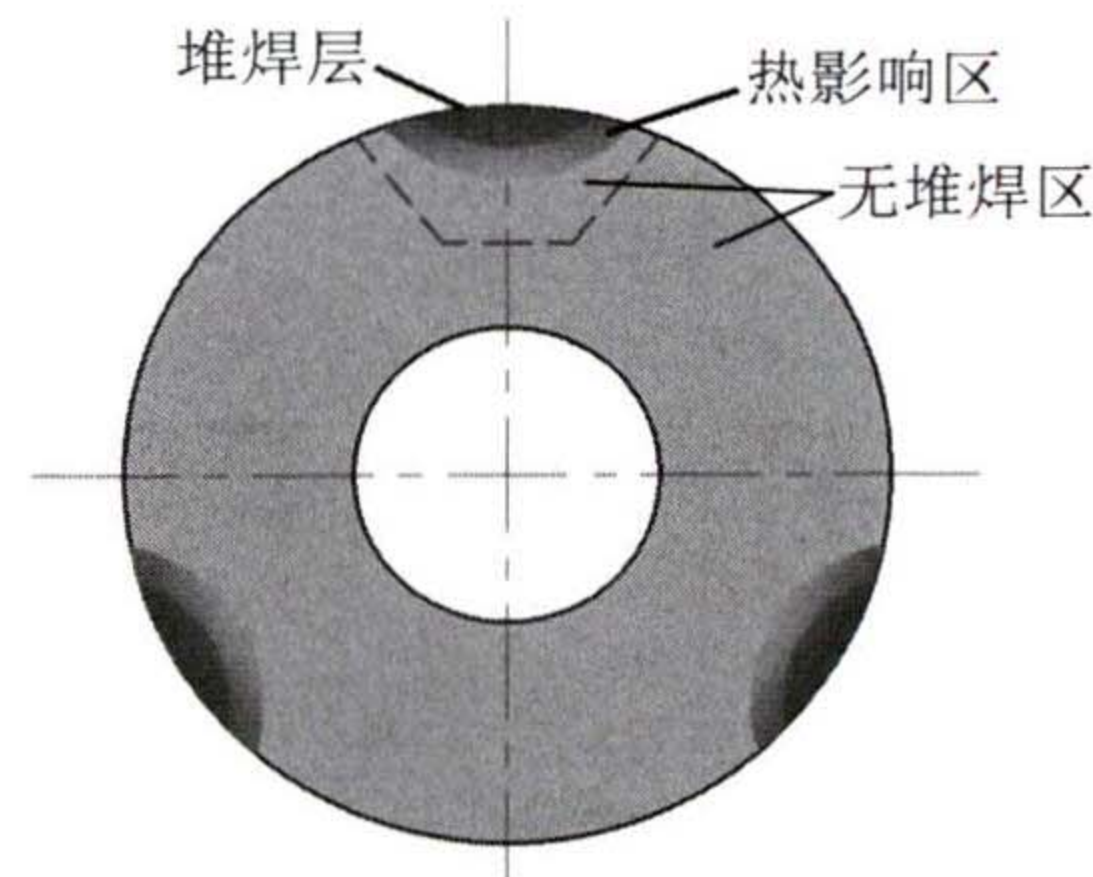


图 2 钢轨试样堆焊位置示意

Fig. 2 Diagram of surfacing positions on rail sample

载列车的轮轨接触状态,根据赫兹接触理论,试验载荷设置为 500 N。钢轨和车轮试样先在干态下循环滚动磨损  $2 \times 10^4$  次,随后在不停机的状态下持续往

接触副中心滴入蒸馏水,水量为  $2.1 \text{ mL} \cdot \text{min}^{-1}$ ,直至试验结束,总循环次数为  $1.5 \times 10^5$  次,试验温度为  $(25 \pm 1)^\circ\text{C}$ ,相对湿度为  $(60 \pm 2)\%$ 。干/湿工况连续磨损可以加速裂纹扩展,以便更好地分析试样损伤情况<sup>[19]</sup>。

磨损试验后,采用线切割法在局部堆焊钢轨试样上截取包含堆焊层、热影响区和无堆焊区的剖面试样,经镶样、打磨、抛光并用体积分数 4% 硝酸酒精溶液腐蚀处理后,使用 OLYMPUS BX53M 型光学显微镜(OM)观察显微组织和裂纹形貌。使用 Hitachi SU8010 型冷场发射扫描电子显微镜(SEM)观察表面和剖面形貌。采用 Zygo ZeGageTM Pro HR 型光学三维轮廓仪观察磨损表面三维形貌,得到表面粗糙度  $R_a$ 。采用 Anton Paar NHT<sup>3</sup> 型纳米力学测试系统对局部堆焊钢轨试样堆焊层、热影响区和无堆焊区进行纳米压痕试验,作用力为 30 mN,保载时间为 10 s,得到硬度。

## 2 试验结果与讨论

### 2.1 黏着系数

车轮踏面所受到的摩擦力与车轮踏面和钢轨接触面间的法向载荷之比称为黏着系数。由图 3 可以看出:在滚动接触磨损过程中,未堆焊和局部堆焊钢轨试样黏着系数的变化趋势基本一致,干态磨损阶段下的黏着系数保持在 0.60 左右,进入湿态磨损阶段后黏着系数瞬时下降至 0.25 左右;干态磨损阶段未堆焊和局部堆焊钢轨试样的平均黏着系数分别为 0.59 与 0.62,局部堆焊钢轨试样的平均黏着系数略高,湿态磨损阶段未堆焊和局部堆焊钢轨试样的平均黏着系数分别为 0.28 与 0.23,局部堆焊钢轨试样的平均黏着系数略低。可见钢轨堆焊提高了干态下轮轨滚动接触界面间的黏着能力,但降低了湿态下轮轨间的黏着能力。

局部堆焊导致钢轨试样沿其周向存在明显硬度差异,堆焊层和热影响区的表面硬度明显高于无堆焊区硬度,如图 4 所示;这种硬度差异易引起钢轨沿周向的非均匀磨损。堆焊层因硬度较高,与车轮试样接触时接触斑的面积相对更大,而更大的接触斑面积会提高轮轨间的黏着系数,故干态下局部堆焊钢轨的黏着系数比未堆焊钢轨略高<sup>[20]</sup>。当滚动磨损工况从干态进入湿态后,水分会进入钢轨试样的裂纹中,在循环接触的挤压作用下加速裂纹的扩展,导致其材料去除能力得到提高<sup>[19]</sup>;较强的材料去除能

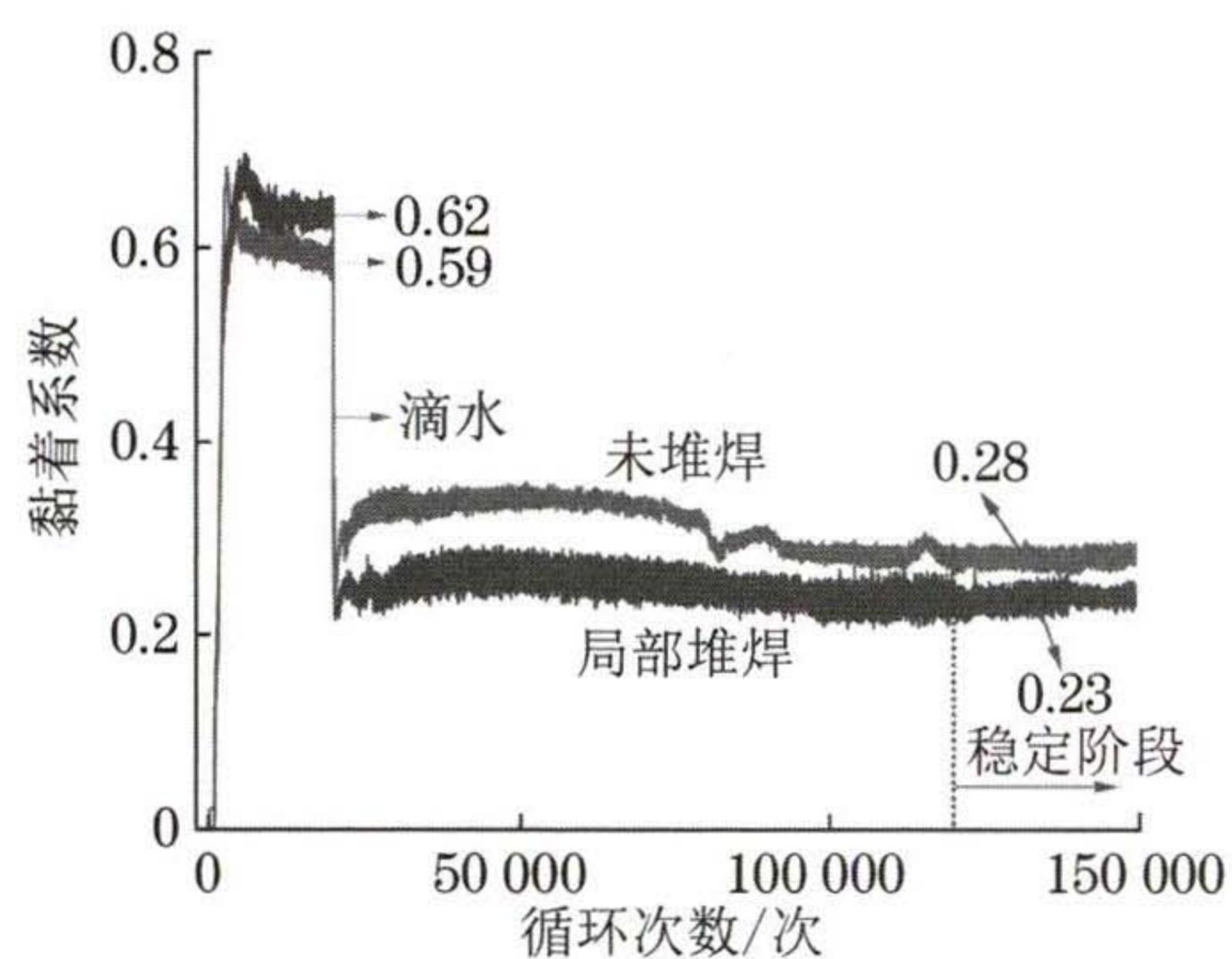


图3 滚动接触磨损过程中未堆焊和局部堆焊钢轨试样的黏着系数变化曲线

Fig. 3 Variation curves of adhesion coefficient of rail samples without surfacing and with local surfacing in rolling contact wear

力使得轮轨接触界面存在较多的磨屑,而更多的磨屑与润滑介质水的混合会更利于降低轮轨间的黏着系数,因此湿态磨损阶段的黏着系数降低。局部堆焊钢轨试样周向存在硬度差,并且堆焊层的硬度明显增大,因此其周向材料的去除能力不一致,同时车轮试样的磨损加剧,使得轮轨之间存在相对更多的磨屑,导致其黏着系数相对更低,并且黏着系数的波动幅度也相对更大。根据文献[21],湿态下局部堆焊钢轨 0.23 的黏着系数仍能保证轮轨间的正常牵引。

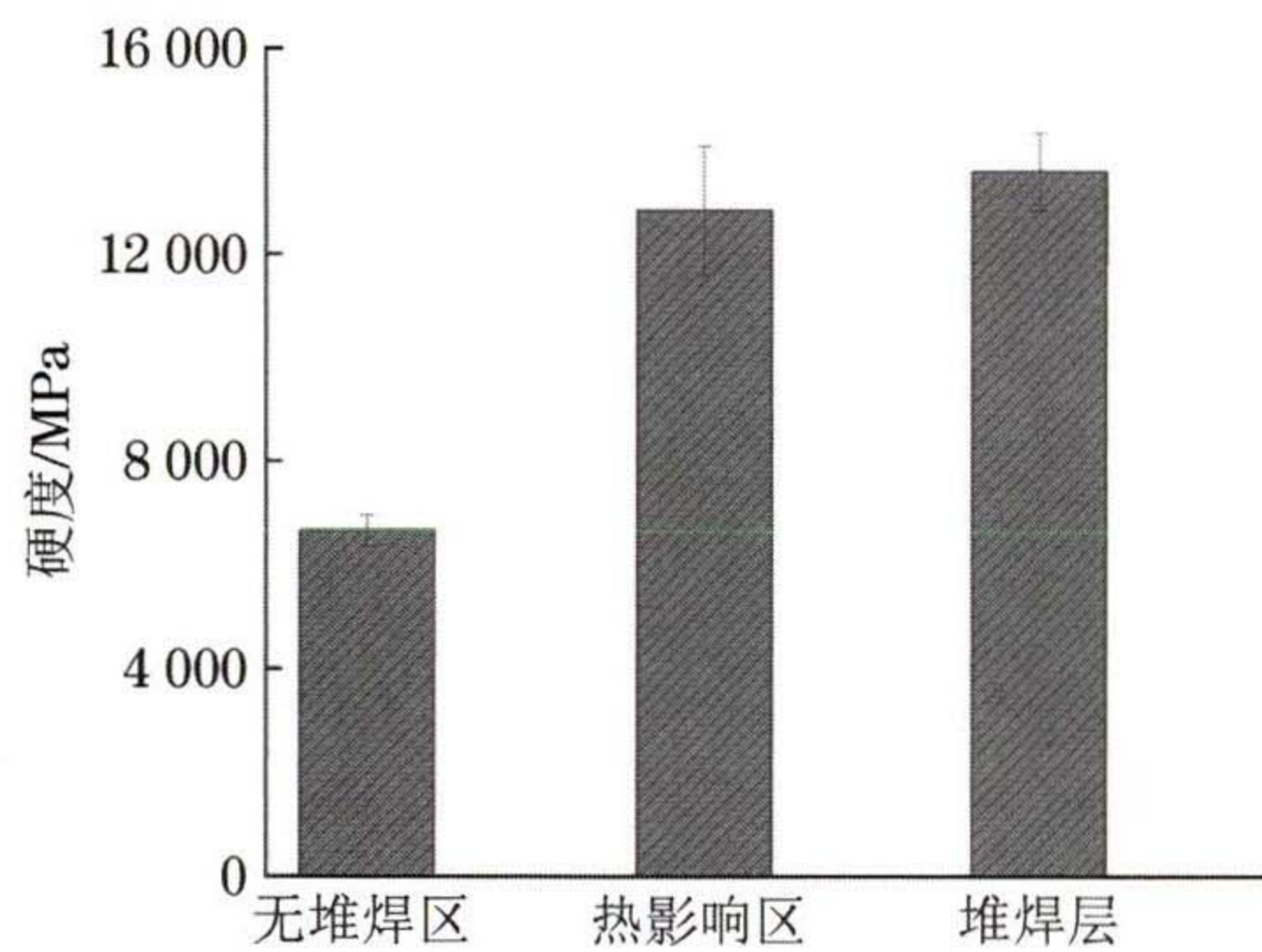


图4 局部堆焊钢轨试样不同区域的纳米硬度

Fig. 4 Nanohardness in different regions of local surfacing rail sample

### 2.2 表面磨损形貌

由图 5 可见:局部堆焊钢轨试样无堆焊区的磨损表面相对平坦,损伤均匀,呈薄片状堆积特征;热影响区的磨损表面坑洼,剥落层厚且不连续,局部出现明显裂纹特征;堆焊层的磨损表面损伤轻微,剥落特征明显减弱。钢轨的磨损与其硬度息息相关<sup>[22]</sup>:堆焊层硬度较高,故损伤最轻微;无堆焊区硬度较低,磨损加剧;热影响区硬度相比于堆焊层略微下降,但不同区域硬度差值增大(由图 4 中误差棒可知),导致损伤最为严重。由图 5(e)还可发现,热影响区的磨损表面具有高低起伏特征,明显存在更深

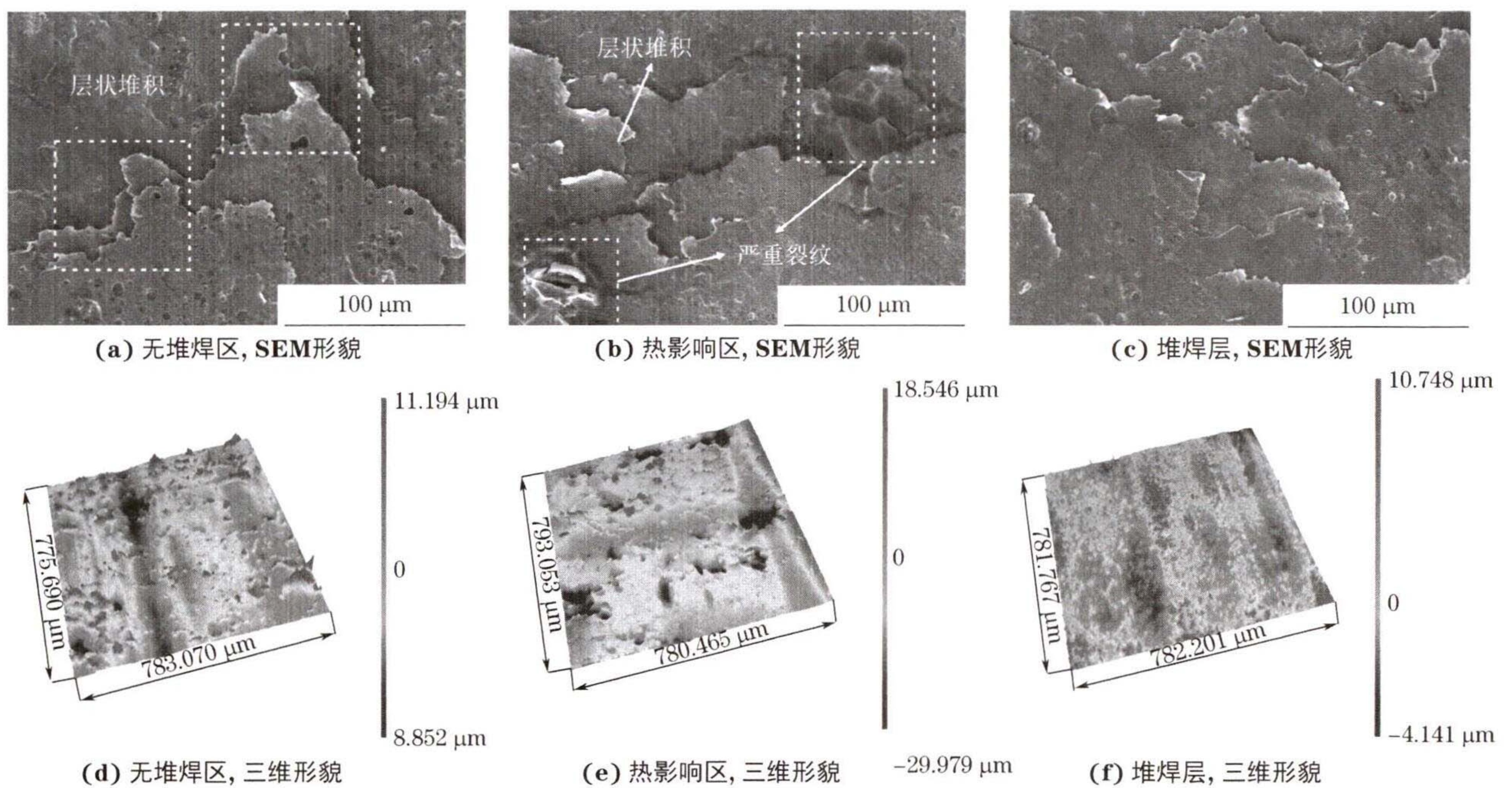


图5 磨损后局部堆焊钢轨试样不同区域的SEM和三维形貌

Fig.5 SEM (a-c) and three-dimensional (d-f) morphology of different regions of local surfacing rail sample after wear:

(a, d) non-surfacing zone; (b, e) heat affected zone and (c, f) surfacing layer

的凹坑。测得滚动接触磨损后,钢轨试样无堆焊区、热影响区与堆焊层的  $R_a$  分别为 0.62, 0.71, 0.30  $\mu\text{m}$ ;这说明热影响区表面因材料去除而更加凹凸不平,磨损相对更加严重。

### 2.3 磨损后剖面形貌

由图6可见:局部堆焊钢轨试样无堆焊区主要

由珠光体组成,堆焊层主要由马氏体组成,热影响区的铁素体、珠光体与马氏体等组织混合不均,热影响区与堆焊层存在较明显的界面。无堆焊区的塑性变形较为明显,裂纹扩展角度相对较小,裂纹扩展至一定深度后折向表面(此处损伤与远离堆焊区域的损伤呈现一致性);堆焊层未出现明显塑性变形和明显

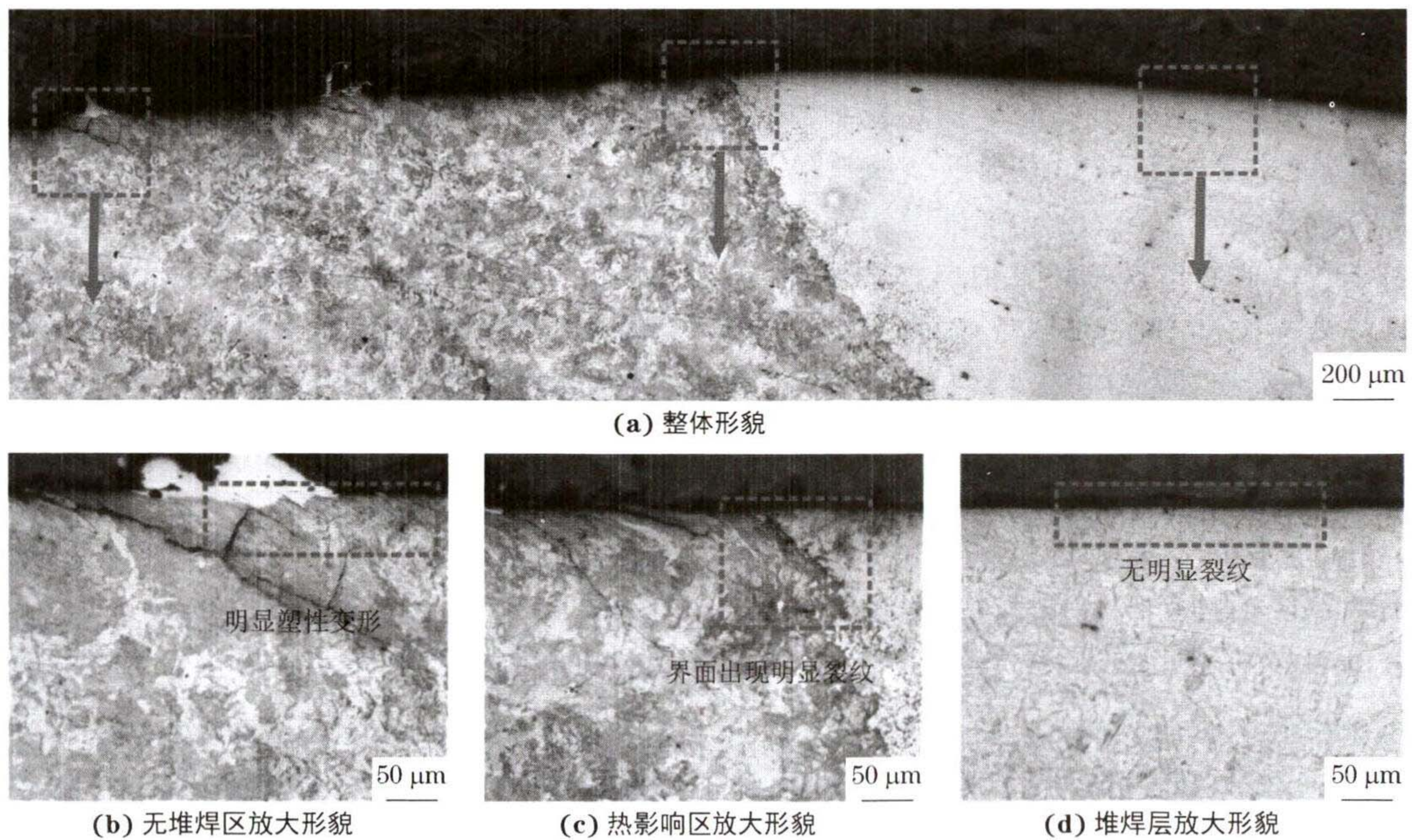


图6 磨损后局部堆焊钢轨试样的剖面OM形貌

Fig.6 OM morphology of cross-section of local surfacing rail sample after wear: (a) overall morphology; (b) enlarged view of non-surfacing zone; (c) enlarged view of heat affected zone and (d) enlarged view of surfacing layer

裂纹;热影响区塑性变形较大且存在大角度扩展的裂纹。马氏体组织的硬度高于铁素体与珠光体<sup>[23]</sup>,因此主要为马氏体组织的堆焊层硬度最高,其次是混杂有马氏体组织的热影响区,无堆焊区的硬度最低。在滚动接触磨损过程中,硬度较高的堆焊层不易发生塑性变形,硬度较低的无堆焊区更容易发生塑性变形。此外,热影响区中出现大角度扩展的裂纹主要是由于其组织不均匀。

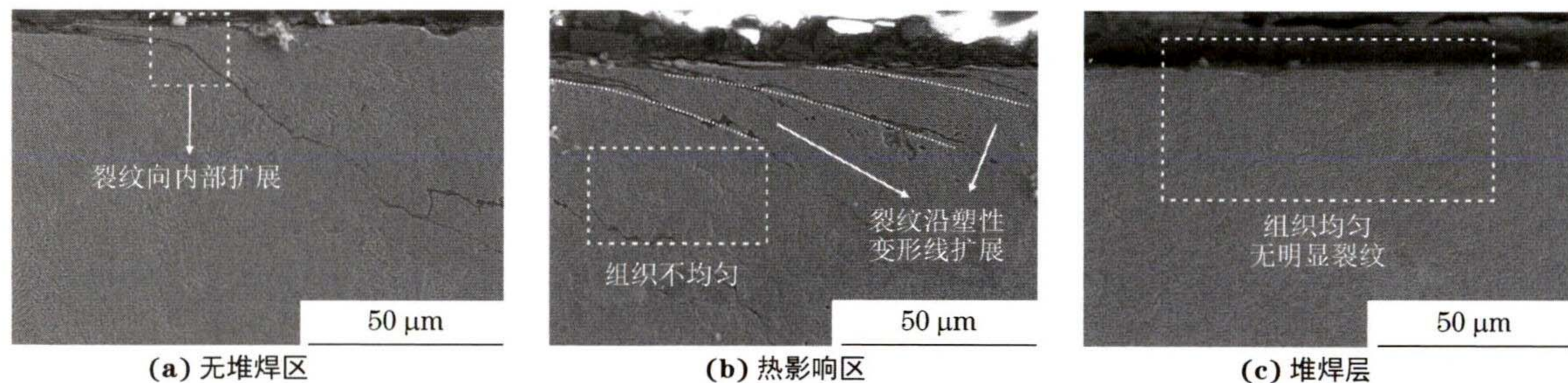


图7 磨损后局部堆焊钢轨试样不同区域的剖面 SEM 形貌

Fig. 7 SEM morphology of cross-section at different regions of local surfacing rail sample after wear: (a) non-surfacing zone; (b) heat affected zone and (c) surfacing layer

### 3 结论

(1) 局部堆焊钢轨试样周向不同区域的组织和硬度不同:堆焊层主要由马氏体组成,硬度最高;热影响区由铁素体、珠光体与马氏体等组织组成,硬度次之;无堆焊区主要由珠光体组成,硬度最小。

(2) 未堆焊和局部堆焊钢轨试样的黏着系数在干态磨损阶段都保持在 0.60 左右,进入湿态磨损阶段则急剧下降,保持在 0.25 左右;干态磨损阶段局部堆焊钢轨试样的黏着系数略高于未堆焊钢轨试样,湿态磨损阶段则相反。

(3) 局部堆焊钢轨试样无堆焊区的磨损表面平坦,损伤均匀,塑性变形较为明显,剖面出现少量裂纹,裂纹萌生初期的扩展角度较小;热影响区的磨损表面更为凹凸不平,磨损表面粗糙度最大,塑性变形较大且出现相对更多的裂纹,裂纹的初始扩展角度也相对更大;堆焊层磨损表面损伤轻微,剥落特征明显减弱,未出现明显塑性变形和明显裂纹。

#### 参考文献:

[1] KABO E. Rolling contact fatigue assessment of repair rail welds[J]. *Wear*, 2019, 436/437: 203030.  
 [2] 高琦. 钢轨表面堆焊修复新技术[J]. *电焊机*, 2012, 42(5): 71-76.  
 GAO Q. Study on a new technology of rail surfacing repairing [J]. *Electric Welding Machine*, 2012, 42(5): 71-76.

由图 7 可以看出:局部堆焊钢轨试样无堆焊区出现少量裂纹,并且裂纹萌生初期的扩展角度较小;热影响区的裂纹相对更多,并且裂纹的初始扩展角度也相对更大;堆焊层则组织均匀,无明显裂纹。堆焊层、热影响区和无堆焊区因组织差异而硬度不同,在滚动磨损过程中承受的应力与应变也不同;而热影响区作为无堆焊区与堆焊层的分界,更容易出现裂纹<sup>[23-24]</sup>。

[3] 陈辉,曾维德,车小莉,等. 铁路在线伤损钢轨堆焊修复新技术研究[J]. *电焊机*, 2004, 34(4): 14-16.  
 CHEN H, ZENG W D, CHE X L, et al. Research on new technology of repairing rails tracks by surfacing welding[J]. *Electric Welding Machine*, 2004, 34(4): 14-16.  
 [4] 朱德稳. 原位焊在核伤钢轨处理中的运用[J]. *铁道运营技术*, 2017, 23(3): 58-60.  
 ZHU D W. Application of in-situ welding in nuclear damaged rail treatment[J]. *Railway Operation Technology*, 2017, 23(3): 58-60.  
 [5] 梁旭,周清跃,张银花,等. 美国钢轨原位修复技术[J]. *中国铁路*, 2019(3): 100-108.  
 LIANG X, ZHOU Q Y, ZHANG Y H, et al. In-situ repair technology of rail in the United States[J]. *China Railway*, 2019(3): 100-108.  
 [6] 王庆伟,陈辉,赵曦. 采用药芯焊丝堆焊修复后的钢轨组织性能[J]. *电焊机*, 2010, 40(1): 79-82.  
 WANG Q W, CHEN H, ZHAO X. Research on microstructure and property of rail by surfacing welding with self-shielded flux-cored wire[J]. *Electric Welding Machine*, 2010, 40(1): 79-82.  
 [7] 陆鑫,李大东,王若愚,等. 焊接工艺对钢轨闪光焊接头性能的影响[J]. *焊接*, 2019(12): 50-55.  
 LU X, LI D D, WANG R Y, et al. Influence of welding process on performance of rail flash butt welded joint[J]. *Welding & Joining*, 2019(12): 50-55.  
 [8] 丁韦,李力,高振坤,等. 贝氏体钢轨闪光焊接技术的研究[J]. *铁道建筑*, 2019, 59(12): 142-146.  
 DING W, LI L, GAO Z K, et al. Research on bainite rail flash butt welding technology [J]. *Railway Engineering*, 2019, 59

- (12):142-146.
- [9] 丁韦,李力,邹定强,等. 贝氏体、珠光体钢轨闪光焊接头力学性能研究[J]. 热加工工艺,2016,45(23):70-73.  
DING W, LI L, ZOU D Q, et al. Study on mechanical properties of flash welding joints of bainite steel and pearlite steel rail[J]. Hot Working Technology,2016,45(23):70-73.
- [10] OSTASH O P, KULYK V V, POZNYAKOV V D, et al. Fatigue crack growth resistance of welded joints simulating the weld-repaired railway wheels metal [J]. Archives of Materials Science and Engineering,2017,2(86):49-52.
- [11] LUCHTENBERG P, DE CAMPOS P T, SOARES P, et al. Effect of welding energy on the corrosion and tribological properties of duplex stainless steel weld overlay deposited by GMAW/CMT process[J]. Surface and Coatings Technology, 2019,375:688-693.
- [12] XU J, WANG P, GAO Y, et al. Geometry evolution of rail weld irregularity and the effect on wheel-rail dynamic interaction in heavy haul railways [J]. Engineering Failure Analysis,2017,81:31-44.
- [13] LI W. Plastic deformation of curved rail at rail weld caused by train-track dynamic interaction [J]. Wear, 2011, 271 (1/2): 311-318.
- [14] CAI W, WEN Z, JIN X, et al. Dynamic stress analysis of rail joint with height difference defect using finite element method [J]. Engineering Failure Analysis, 2007, 14 (8): 1488-1499.
- [15] 究文涛,李晓延,孙建通,等. 钢轨轨面堆焊温度场的数值模拟 [J]. 机械工程材料,2015,39(8):103-106.  
YAN W T, LI X Y, SUN J T, et al. Numerical simulation of temperature field of rail steel overlay welding [J]. Materials for Mechanical Engineering, 2015, 39 (8): 103-106.
- [16] JUN H K, SEO J W, JEON I S, et al. Fracture and fatigue crack growth analyses on a weld-repaired railway rail [J]. Engineering Failure Analysis, 2016, 59: 478-492.
- [17] LIU R F, WANG J C. Finite element analyses of the effect of weld overlay sizing on residual stresses of the dissimilar metal weld in PWRs [J]. Nuclear Engineering and Design, 2021, 372: 110959.
- [18] 高炳易. 贝氏体焊条直接堆焊修复铁路钢轨特性研究 [J]. 热加工工艺, 2009, 38 (11): 138-140.  
GAO B Y. Study on characteristics of bainitic welding rod for direct built-up welding in rail [J]. Hot Working Technology, 2009, 38 (11): 138-140.
- [19] 刘园. 液体对轮轨滚动接触疲劳作用下的钢轨表面裂纹扩展机理的影响 [J]. 上海海事大学学报, 2011, 32 (1): 65-69.  
LIU Y. Effect of liquid penetration on rail crack propagation mechanism under rolling contact fatigue between wheel and rail [J]. Journal of Shanghai Maritime University, 2011, 32 (1): 65-69.
- [20] HU Y, ZHOU L, DING H H, et al. Investigation on wear and rolling contact fatigue of wheel-rail materials under various wheel/rail hardness ratio and creepage conditions [J]. Tribology International, 2020, 143: 106091.
- [21] FOO C T, OMAR B, JALIL A S. A review on recent wheel/rail interface friction management [J]. Journal of Physics: Conference Series, 2018, 1049: 012009.
- [22] 王军平,周宇,沈钢. 钢轨硬度对疲劳裂纹萌生和钢轨磨耗的影响 [J]. 西南交通大学学报, 2021, 56 (3): 611-618.  
WANG J P, ZHOU Y, SHEN G. Effect of rail hardness on fatigue cracks initiation and rail wear [J]. Journal of Southwest Jiaotong University, 2021, 56 (3): 611-618.
- [23] SU Y. The sensitivity analysis of microstructure and mechanical properties to welding parameters for linear friction welded rail steel joints [J]. Materials Science and Engineering: A, 2019, 764: 138251.
- [24] HU Y. Microstructure evolution of railway pearlitic wheel steels under rolling-sliding contact loading [J]. Tribology International, 2021, 154: 106685.
- [28] IMAYEV R M, IMAYEV V M, OEHRING M, et al. Alloy design concepts for refined gamma titanium aluminide based alloys [J]. Intermetallics, 2007, 15 (4): 451-460.
- [29] DING X F, LIN J P, ZHANG L Q, et al. Lamellar orientation control in a Ti-46Al-5Nb alloy by directional solidification [J]. Scripta Materialia, 2011, 65 (1): 61-64.
- [30] BURGERS W G. On the process of transition of the cubic-body-centered modification into the hexagonal-close-packed modification of zirconium [J]. Physica, 1934, 1: 561-586.
- [31] BLACKBURN M J. Some aspects of phase transformations in titanium alloys [M] // Science, Technology and Application of Titanium. London: Oxford Pergamon Press Ltd., 1970: 633-643.

(上接第 13 页)